

Invariance of Weight Distributions in Rectified MLPs

Russell Tsuchida^{*} Farbod Roosta-Khorasani[†] Marcus Gallagher[‡]

July 6, 2022

Abstract

An interesting approach to analyzing and developing tools for neural networks that has received renewed attention is to examine the equivalent kernel of the neural network. This is based on the fact that a fully connected feedforward network with one hidden layer, a certain weight distribution, an activation function, and an infinite number of neurons is a mapping that can be viewed as a projection into a Hilbert space. We show that the equivalent kernel of an MLP with ReLU or Leaky ReLU activations for all rotationally-invariant weight distributions is the same, generalizing a previous result that required Gaussian weight distributions. We derive the equivalent kernel for these cases. In deep networks, the equivalent kernel approaches a pathological fixed point, which can be used to argue why training randomly initialized networks can be difficult. Our results also have implications for weight initialization and the level sets in neural network cost functions.

1 Introduction

Neural networks have recently been applied to a number of diverse problems [4, 27, 36] with impressive results. These breakthroughs largely appear to be driven by application rather than an understanding of the expressive capabilities and training considerations of neural networks. Recently, significant work has been done to increase understanding of neural networks, e.g., [2, 8, 12, 24, 31, 32, 34, 35, 41]. However, there is still work to be done to bring theoretical understanding in line with the results seen in practice.

The connection between neural networks and kernel machines has long been known [26]. Much past work has been done to investigate the equivalent kernel of certain neural networks, either experimentally [6], through sampling [21, 22, 37], or analytically by assuming some random distribution over the weight parameters in the network [1, 7, 10, 28, 29, 40]. Surprisingly, in the latter approach, rarely have distributions other than the Gaussian distribution been analyzed. This is likely due to early influential work on Bayesian Networks [23], which laid a strong mathematical foundation for a Bayesian approach to training networks.

In this work, we investigate the equivalent kernels for networks with Rectified Linear Unit (ReLU) or Leaky ReLU (LReLU) activation functions, one-hidden layer, and more general weight distributions. Our analysis carries over to deep networks. We investigate the consequences that weight initialization has on the equivalent kernel at the beginning of training. While initialization schemes that mitigate exploding/vanishing gradient problems [3, 14, 15] for other activation functions and weight distribution combinations have been explored in earlier works [11, 13], we discuss an initialization scheme for Multi-Layer Perceptrons (MLPs) with LReLUs and weights coming from a rotationally-invariant distribution. The derived kernels also allow us to analyze the loss of information as an input is propagated through the network, offering a complementary view to the shattered gradient problem [2]. Finally, we use our analysis to comment on the nature of some of the level sets in MLPs. Our result has three main implications:

1. The equivalent kernel in randomized (L)ReLU MLPs converges to a function $k(\mathbf{x}, \mathbf{y}) \propto \|\mathbf{x}\|\|\mathbf{y}\|$ as the number of layers grows. The utility of this kernel is obviously very limited. This makes the network difficult to train in initial stages for a wide class of optimizers.
2. To preserve the signal norm in a ReLU network, the variance should be chosen appropriately. This result was previously described in [13], but only the Gaussian distribution was considered for initialization. Our results show that any rotationally-invariant weight distribution results in the same equivalent kernel. The variance required to preserve norms in LReLU networks has also been found.
3. In addition to the obvious permutation symmetry that exists in MLPs, level sets can be considered by noting that the equivalent kernel of a (L)ReLU MLP is the same for rotationally-invariant weight distributions.

^{*}School of ITEE, University of Queensland, Brisbane, Australia, Email: s.tsuchida@uq.edu.au

[†]School of Mathematics and Physics, University of Queensland, Brisbane, Australia, and International Computer Science Institute, Berkeley, USA, Email: fred.roosta@uq.edu.au

[‡]School of ITEE, University of Queensland, Brisbane, Australia, Email: marcusg@uq.edu.au

2 Preliminaries

Consider a feedforward neural network with an input layer with m neurons and a hidden layer with n neurons. Let $\sigma_1 \equiv \sigma_2 \equiv \dots \equiv \sigma_n \equiv \sigma$ with $\sigma : \mathbb{R} \rightarrow \mathbb{R}$ be the activation function of all the neurons in the hidden layer. We have a single hidden layer network, as shown in Figure 1.

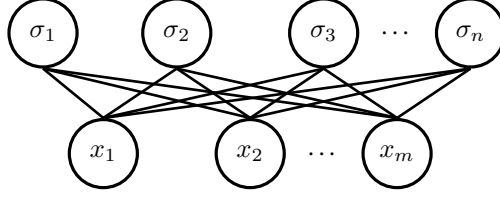


Figure 1: A fully connected feedforward network with one hidden layer.

Further assume that the biases are 0, as is common when initializing neural network parameters. Taking any two inputs $\mathbf{x} \in \mathbb{R}^m$ and $\mathbf{y} \in \mathbb{R}^m$ and feeding them through the network, the dot product in the hidden layer is

$$\frac{1}{n} \mathbf{h}(\mathbf{x}) \cdot \mathbf{h}(\mathbf{y}) = \frac{1}{n} \sum_{i=1}^n \sigma(\mathbf{w}_i \cdot \mathbf{x}) \sigma(\mathbf{w}_i \cdot \mathbf{y}), \quad (1)$$

where $\mathbf{h}(\cdot)$ denotes the n dimensional vector in the hidden layer and $\mathbf{w}_i \in \mathbb{R}^m$ is the weight vector into the i^{th} neuron. Assuming an infinite number of hidden neurons, the sum in (1) has an interpretation as an inner product in feature space, which corresponds to the kernel of a Hilbert space. We have

$$\begin{aligned} k(\mathbf{x}, \mathbf{y}) &= \int_{\mathbb{R}^m} \sigma(\mathbf{w} \cdot \mathbf{x}) \sigma(\mathbf{w} \cdot \mathbf{y}) \mathbf{d}\mathbb{P}(\mathbf{w}) \\ &= \int_{\mathbb{R}^m} \sigma(\mathbf{w} \cdot \mathbf{x}) \sigma(\mathbf{w} \cdot \mathbf{y}) f(\mathbf{w}) \mathbf{d}\mathbf{w}, \end{aligned} \quad (2)$$

where $\mathbb{P}(\mathbf{w})$ is an appropriate probability measure with its Radon–Nikodym derivative with respect to the Lebesgue measure, i.e., the probability density function (PDF), $f(\mathbf{w})$, for the identically distributed weight vector $\mathbf{W} = (W_1, \dots, W_m)^T$ in the network. The connection of (2) to the kernels in kernel machines is well known [7, 26, 40].

3 Equivalent Kernels of Infinite Hidden Layers

The kernel (2) has previously been evaluated for a number of choices of f and σ . The known kernels are summarized in Table 1.

Table 1: Known equivalent kernels.

	Gaussian	Uniform
Gaussian	✓	
Sigmoid	✓	
sgn		✓
ReLU	✓	

In particular, the equivalent kernel for a one-hidden layer network with Gaussian distributed weights of variance σ_W^2 and mean 0 is the Arc-Cosine Kernel [7]

$$k(\mathbf{x}, \mathbf{y}) = \frac{\sigma_W^2 \|\mathbf{x}\| \|\mathbf{y}\|}{2\pi} (\sin \theta_0 + (\pi - \theta_0) \cos \theta_0), \quad (3)$$

where $\theta_0 = \cos^{-1} \left(\frac{\mathbf{x} \cdot \mathbf{y}}{\|\mathbf{x}\| \|\mathbf{y}\|} \right)$ is the angle between the inputs \mathbf{x} and \mathbf{y} . Noticing that the Arc-Cosine Kernel $k(\mathbf{x}, \mathbf{y})$ depends on \mathbf{x} and \mathbf{y} only through their norms, with an abuse of notation we will henceforth set

$$k(\mathbf{x}, \mathbf{y}) \equiv k(\theta_0).$$

Define the *normalized kernel* to be the cosine similarity between the signals in the hidden layer. The normalized Arc-Cosine Kernel is given by

$$\cos \theta_1 = \frac{k(\mathbf{x}, \mathbf{y})}{\sqrt{k(\mathbf{x}, \mathbf{x})} \sqrt{k(\mathbf{y}, \mathbf{y})}} = \frac{1}{\pi} (\sin \theta_0 + (\pi - \theta_0) \cos \theta_0),$$

where θ_1 is the angle between the signals in the first layer. Figure 2 shows a plot of the normalized Arc-Cosine Kernel.

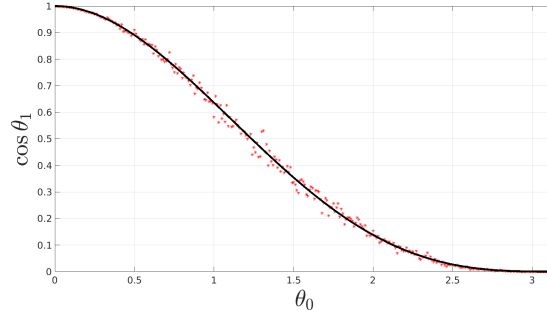


Figure 2: normalized kernel as a function of θ_0 for a single hidden layer network, Gaussian weights, and ReLU activations. Empirical samples from a network with 1000 inputs and 1000 hidden units are plotted alongside the theoretical ideal curve. Each sample is obtained by generating R from a QR decomposition of a random matrix, then setting $\mathbf{x} = R^T(1, 0, \dots, 0)^T$ and $\mathbf{y} = R^T(\cos \theta, \sin \theta, 0, \dots, 0)^T$.

A reasonable question to ask is how the equivalent kernel changes for a different choice of weight distribution. The equivalent kernel for networks with (L)ReLU activations and general rotationally-invariant weight distributions is investigated in Section 4 and 5.

The equivalent kernel can be composed and applied to deep networks. The kernel can also be used to choose good weights for initialization. These, as well as other implications for practical neural networks, are investigated in Section 6.

Our work is closely related to [31,34]. However, our results apply to the unbounded (L)ReLU activation function and more general weight distributions, and their work considers random biases as well as weights.

4 Equivalent Kernel for Rotationally-Invariant Distributions

In this section we present our main theoretical results.

Proposition 1 (Equivalent Kernel as a Solution to a Second Order Initial Value Problem)

Suppose we have a one-hidden layer feedforward network with ReLU activation functions and random identically distributed weights with PDF $f : \mathbb{R}^m \rightarrow \mathbb{R}$. For inputs $\mathbf{x}, \mathbf{y} \in \mathbb{R}^m$ the equivalent kernel of the network is the solution to the Initial Value Problem (IVP)

$$\frac{d^2 k(\theta)}{d\theta_0^2} + k(\theta_0) = F(\theta_0), \quad k'(\pi) = 0, \quad k(\pi) = 0 \quad (4)$$

where θ_0 is the angle between the inputs \mathbf{x} and \mathbf{y} . $F(\theta_0)$ is given by the $m - 1$ dimensional integral

$$F(\theta_0) = \int_{\mathbb{R}^{m-1}} f\left(R(s \sin \theta_0, -s \cos \theta_0, w_3, \dots, w_m)^T\right) \Theta(s) s^3 ds dw_3 dw_4 \dots dw_m \|\mathbf{x}\| \|\mathbf{y}\| \sin \theta_0, \quad (5)$$

where R is an orthogonal matrix, and Θ is the Heaviside step function.

The proof is given in Appendix A. A rough idea of the proof is as follows. Firstly, following [7], rotate the \mathbf{w} coordinate system so that

$$k(\mathbf{x}, \mathbf{y}) = \int_{\mathbb{R}^m} \Theta(w_1) \Theta(w_1 \cos \theta_0 + w_2 \sin \theta_0) w_1 (w_1 \cos \theta_0 + w_2 \sin \theta_0) f(R\mathbf{w}) d\mathbf{w} \|\mathbf{x}\| \|\mathbf{y}\|.$$

Now differentiating twice with respect to θ_0 yields the second order ODE (4).

The ODE in (4) has a physical interpretation as a second order circuit with θ_0 replacing time, as shown in Figure 3.

The usefulness of the ODE in its current form is limited, since the forcing term $F(\theta_0)$ as in (5) is difficult to interpret. Remarkably, however, regardless of the underlying distribution on weights \mathbf{w} , as long as the PDF f in (5) corresponds to any rotationally-invariant distribution, the integral enjoys a much simpler representation.

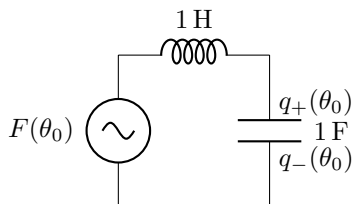


Figure 3: Equivalent kernel ODE as an equivalent LC circuit. The circuit contains a unit inductor, unit capacitor and voltage source $F(\theta_0)$. The kernel $k(\theta_0)$ is the charge across the capacitor $k(\theta_0) = q_+(\theta_0) - q_-(\theta_0)$.

Proposition 2 (Forcing Term for Rotationally-Invariant Distributions)

Suppose the weights W_i are uncorrelated and identically distributed with some rotationally-invariant distribution $f(\mathbf{w}) = f(O\mathbf{w})$ for all orthogonal matrices $O \in \mathcal{O}(n)$. The forcing term $F(\theta_0)$ in the kernel ODE is given by

$$F(\theta_0) = \frac{\mathbb{E}[W_i^2]}{\pi} \|\mathbf{x}\| \|\mathbf{y}\| \sin \theta_0. \quad (6)$$

The proof is given in Appendix B. A rough idea of the proof is as follows. Find the coefficient of $\sin \theta_0$ in the Fourier series expansion of $F(\theta_0)$. Using the rotational invariance of f , show that $F(\theta_0)$ is a constant multiple of $\sin \theta_0$. By orthogonality, the constant corresponds to the Fourier coefficient of $\sin \theta_0$.

In our physical connection to the equivalent circuit, the voltage source is (6) for any rotationally-invariant f . Recall that the class of rotationally-invariant distributions [5], as a subclass of elliptically contoured distributions [18], includes the Gaussian distribution, the multivariate t-distribution, the symmetric multivariate Laplace distribution, and symmetric multivariate stable distributions.

The remarkable feature of the representation (6) of the forcing term (5) in (4) is that the underlying distribution appears only as the second moment, $\mathbb{E}[W_i^2]$. In other words, for all rotationally invariant distributions with the same second moment, the forcing term in (4) is the same, implying the *same equivalent kernel*. More formally, we can combine Propositions 1 and 2 to find the equivalent kernel assuming rotationally-invariant weight distributions.

Corollary 3 (Equivalent Kernel Rotationally-Invariant Distributions, ReLU)

Suppose we have a one-hidden layer feedforward network with ReLU activation functions and uncorrelated and identically distributed random weights with rotationally-invariant PDF $f : \mathbb{R}^m \rightarrow \mathbb{R}$. The equivalent kernel of the network is

$$k(\mathbf{x}, \mathbf{y}) = \frac{\|\mathbf{x}\| \|\mathbf{y}\| \mathbb{E}[W_i^2]}{2\pi} (\sin \theta_0 + (\pi - \theta_0) \cos \theta_0). \quad (7)$$

This is easily obtained by solving the IVP in Proposition 1 using the forcing term from Proposition 2. The corresponding normalized kernel is again

$$\cos \theta_1 = \frac{1}{\pi} (\sin \theta_0 + (\pi - \theta_0) \cos \theta_0).$$

This result extends an earlier result [7], which only considers the weights from a Gaussian distribution.

One can apply the same technique to the case of LReLU activations $\sigma(z) = (a + (1 - a)\Theta(z))z$ where a is the negative gradient parameter. The factor of $\sigma(\mathbf{w} \cdot \mathbf{x})\sigma(\mathbf{w} \cdot \mathbf{y})$ in (2) can be expanded, resulting in four integrals. The four integrals can, in turn, be converted to four ODEs, and hence, (2) can be solved using superposition. Noting that it is just a slightly more involved calculation than the ReLU case, we defer our proof to Appendix C.

Also note that a single layer LReLU network does not strictly have an equivalent kernel, since it is naturally implicit that a kernel must be positive semi-definite (PSD). Nevertheless, with LReLU activations and weights coming from a rotationally-invariant distribution, the integral in (2) has an equivalent form.

Corollary 4 (Equivalent “Kernel” Rotationally-Invariant Distributions, LReLU)

Suppose we have a one-hidden layer feedforward network with LReLU activation functions and uncorrelated and identically distributed random weights with rotationally-invariant PDF $f : \mathbb{R}^m \rightarrow \mathbb{R}$. The integral (2) is

$$k(\mathbf{x}, \mathbf{y}) = \left[\frac{(1-a)^2}{2\pi} (\sin \theta_0 + (\pi - \theta_0) \cos \theta_0) + a \cos \theta_0 \right] \mathbb{E}[W_i^2] \|\mathbf{x}\| \|\mathbf{y}\|,$$

where $a \in (0, 1)$ is the LReLU gradient parameter.

The corresponding normalized “kernel” is

$$\cos(\theta_1) = \frac{1}{1+a^2} \left[\frac{(1-a)^2}{\pi} (\sin \theta_0 + (\pi - \theta_0) \cos \theta_0) + 2a \cos \theta_0 \right].$$

While a one-hidden layer LReLU network’s kernel cannot be PSD (with $a > 0$), note that a multi-hidden layer network’s kernel may be PSD (see Figure 5).

5 Empirical Verification of Results

We now empirically verify the theoretical results presented in Section 4.

5.1 Empirical Verification of Proposition 2

Figure 4 shows Monte Carlo estimates of the forcing term (5) and the simple representation given by Proposition 2. We consider the m dimensional t-distribution

$$f(\mathbf{w}) = \frac{\Gamma[(\nu + m)/2]}{\Gamma(\nu/2)\nu^{m/2}\pi^{m/2}\sqrt{|\det(\Sigma)|}} \left[1 + \frac{1}{\nu}(\mathbf{w}^T \Sigma^{-1} \mathbf{w}) \right]^{-(\nu+m)/2},$$

with degrees of freedom ν and diagonal shape matrix $\Sigma = I$. Random samples are scaled to have a variance of $\sigma_W^2 = 0.1$. The t-distribution approaches the Gaussian as $\nu \rightarrow \infty$. To estimate the integral in (5) when f is the t-distribution, we numerically integrate (12) (derived in Appendix B).

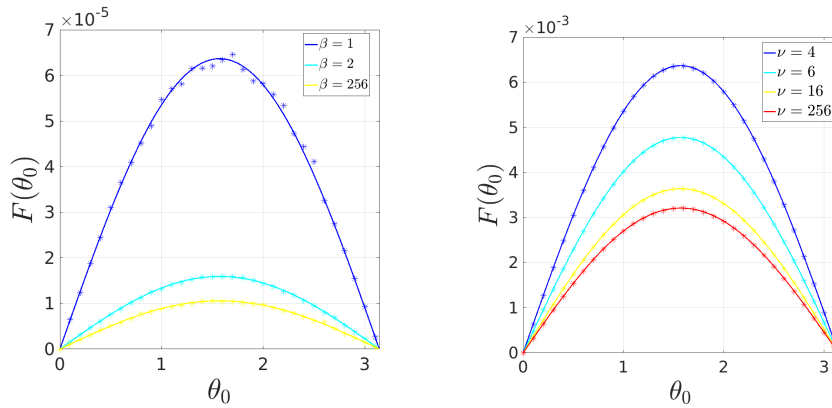


Figure 4: Analytical forcing term (solid line) with Monte Carlo estimates of forcing term (points). Each Monte Carlo sample is an empirical estimate of the expectation using 10^6 samples. (Left) Samples from the distribution (8) with $\alpha = 0.01$. The sampling process for each θ_0 is as described in Figure 2, with the modification that $m = 100$. (Right) Samples from the t-distribution.

We also plot samples from the multivariate distribution

$$f(\mathbf{w}) = \prod_{i=1}^m \frac{\beta}{2\alpha\Gamma(1/\beta)} e^{-|w_i/\alpha|^\beta}, \quad (8)$$

which is not rotationally-invariant in general. To estimate the integral in (5) for this distribution, we considered the following equivalent form, which is more amenable for use in many off-the-shelf software packages,

$$F(\theta_0) = \mathbb{E} \left[f(\boldsymbol{\gamma} \cdot \mathbf{W}_{m-1}) (|(\mathbf{W}_{m-1} \cdot \mathbf{t}_1^{-1})^3| + (\mathbf{W}_{m-1} \cdot \mathbf{t}_1^{-1})^3) \right] \frac{\sin \theta_0}{2|\det(T_{m-1})|} \|\mathbf{x}\| \|\mathbf{y}\|.$$

We refer the reader to Appendix D for derivation and explanation of the symbols in this expression.

For the t-distribution, the empirical samples closely follow the theoretical curve. It is curious that Proposition 2 for the forcing term seems to approximately hold for the distribution (8), despite the fact that this distribution is not rotationally-invariant. In light of this empirical observation, we conjecture that the universality of the forcing term holds in an approximate sense more generally than for the case of rotationally-invariant distributions.

5.2 Empirical Verification of Corollary 3 and 4

In Figure 5, we empirically verify Corollary 3 and 4. In the one hidden layer case, the samples follow the blue curve, regardless of the weight distribution which varies with ν . Once again, we observe that the universality of the equivalent kernel appears to hold for the (8) distribution.

6 Implications for Real Networks

6.1 Composed Kernels in Deep Networks

A recent advancement in understanding the difficulty in training deep neural networks is the identification of the shattered gradients problem [2]. Without skip connections, the gradients of deep networks approach white noise as they are backpropagated through the network, making them difficult to train.

A simple observation that complements this view is obtained through repeated composition of the normalized kernel. The angle between two inputs in the j^{th} layer of a ReLU network with symmetric weights and a large number of inputs is approximately

$$\cos \theta_j = \frac{1}{\pi} (\sin \theta_{j-1} + (\pi - \theta_{j-1}) \cos \theta_{j-1}).$$

A result similar to the following is hinted at in [21], citing [34]. Their analysis, which considers biases in addition to weights [31], yields insights on the trainability of random neural networks that our analysis cannot. However, their argument does not appear to provide a complete formal proof for the case when the activation functions are unbounded, e.g., ReLU. The degeneracy of the composed kernel with more general activation functions is also proved in [10], with the assumption that the weights are Gaussian distributed.

Corollary 5 (Fixed Point of Normalized Kernel, LReLU, ReLU)

The normalized kernel obtains a unique fixed point at $\theta^ = 0$.*

Proof. For $a = 0$, let $z = \cos \theta_{j-1}$ and define $T(z) = \frac{1}{\pi} (\sqrt{1 - z^2} + (\pi - \cos^{-1} z)z)$. The magnitude of the derivative of T is $|1 - \frac{\cos^{-1} z}{\pi}|$ which is bounded above by 1 on $[-1, 1]$. Therefore, T is a contraction mapping. By Banach’s fixed point theorem there exists a *unique* fixed point $z^* = \cos \theta^*$ with $\cos \theta^* = \frac{1}{\pi} (\sin \theta^* + (\pi - \theta^*) \cos \theta^*)$. Set $\theta^* = 0$ to verify that $\theta^* = 0$ is a solution, and θ^* is unique.

For $a \neq 0$, set T appropriately and note that the derivative of T is the same as the case when $a = 0$. \square

Corollary 5 implies that for this deep network, the angle between the signals at a deep layer for any two input signals approaches 0! In other words, no matter what the input is, the kernel “sees” the same thing after accounting for the scaling induced by the norm of the input. Hence, it becomes increasingly more difficult to train deeper networks, as much of the information is lost and the outputs will depend merely on the norm of the inputs.

At first this may seem counter-intuitive. An appeal to intuition can be made by considering the corresponding linear network, which amounts to the celebrated power iteration method. In this case, the repeated application of a matrix transformation A to a vector v converges to the dominant eigenvector (i.e. the eigenvector corresponding to the largest eigenvalue) of A .

Figure 5 shows the theoretical normalized kernel for networks of increasing depth with empirical samples from randomly initialized neural networks.

Contrary to the shattered gradients analysis, which applies to gradient based optimizers, our analysis shows that any optimizer that initializes or samples weights from some rotationally-invariant distribution will experience problems due to the loss of information as the signal propagates through the network.

6.2 Initialization

Corollary 6 (Norm Preserving Variance, ReLU)

Let \mathbf{x} be the input to a hidden layer containing ReLU activations with uncorrelated and identically distributed weights W coming from a rotationally-invariant distribution and let $\mathbf{h}(\mathbf{x})$ be the signal in the hidden layer. To approximately preserve the ℓ_2 norm (requiring $\|\mathbf{h}(\mathbf{x})\| = \|\mathbf{x}\|$), we have that

$$\sqrt{\mathbb{E}[W^2]} = \sqrt{\frac{2}{n}}, \tag{9}$$

where n is the number of neurons in the hidden layer.

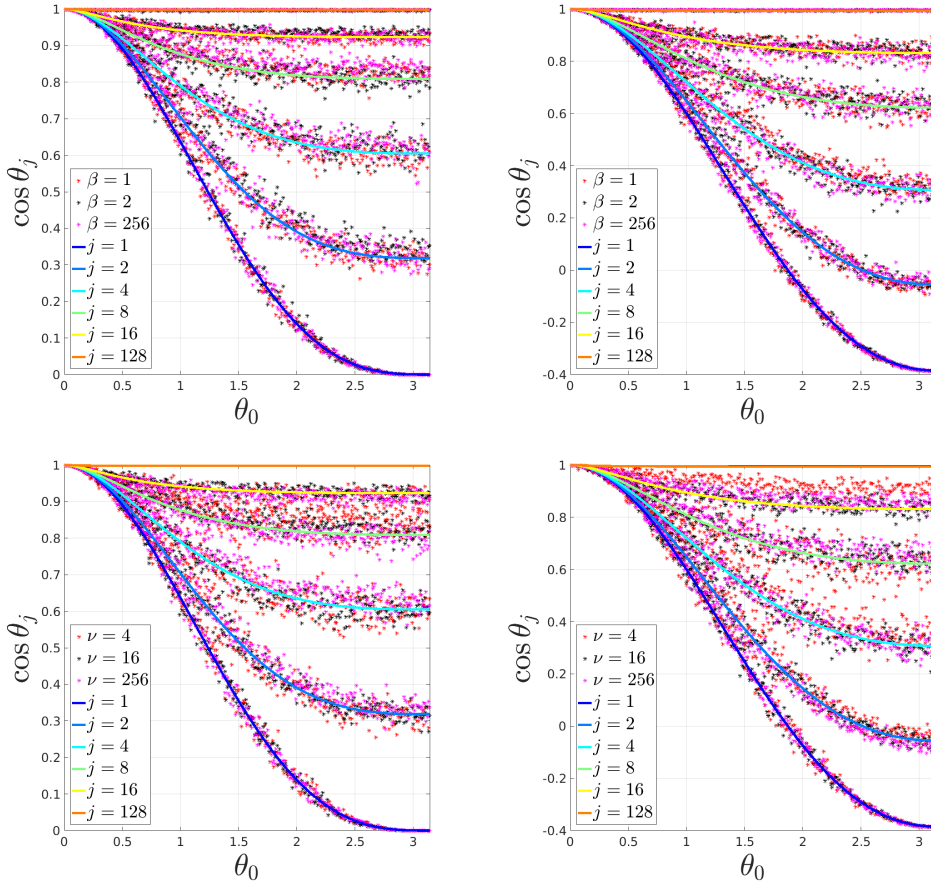


Figure 5: Theoretical normalized kernel for networks of increasing depth. Empirical samples from a network with between 1 and 128 hidden layers, 1000 hidden neurons in each layer, $m = 1000$ and weights coming from different symmetric distributions. The sampling process for each θ_0 is as described in Figure 2. (Top Left) ReLU Activations, (8) distribution. (Top Right) LReLU Activations with $a = 0.2$, (8) distribution. (Bottom Left) ReLU Activations, t-distribution. (Bottom Right) LReLU Activations with $a = 0.2$, t-distribution.

Proof. The ℓ_2 -norm of the signal in a one hidden layer network with ReLU activation functions, n neurons and symmetric distributions for an input \mathbf{x} is approximately $\|\mathbf{h}(\mathbf{x})\| = \sqrt{k(\mathbf{x}, \mathbf{x})n}$, as evident by the definition in (2). Letting $\theta_0 = 0$ in (7), we have

$$\|\mathbf{h}(\mathbf{x})\| = \|\mathbf{x}\| \sqrt{\frac{n\mathbb{E}[W_i^2]}{2}}.$$

Setting $\|\mathbf{h}(\mathbf{x})\| = \|\mathbf{x}\|$ completes the proof. \square

This agrees with the well-known case when W comes from a Gaussian distribution [13]. However, according to our analysis, we see no reason why W should be restricted to come from a Gaussian distribution. The equivalent kernel of a ReLU network is the same for the class of rotationally-invariant distributions. According to our empirical observation, when the weights come from a Laplace distribution $f(w) = \frac{1}{2b}e^{-|w|/b}$, choosing

$$b = \sqrt{\frac{1}{n}}$$

preserves the signal norms. When the weights come from a uniform distribution on $[-a, a]$, choosing

$$a = \sqrt{\frac{6}{n}}$$

preserves the signal norms.

Corollary 7 (Norm Preserving Variance, LReLU)

Consider a hidden layer containing LReLU activations with gradient parameter $a \in (0, 1)$ and uncorrelated

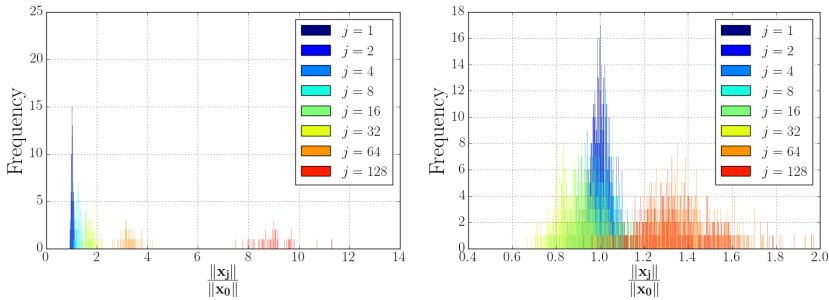


Figure 6: Histograms showing the ratio of the norm of signals in layer j to the norm of the input signals. Each histogram contains 1000 data points randomly sampled from a unit Gaussian distribution. The network tested has 1000 inputs, 1000 neurons in each layer, and LReLU activations with $a = 0.2$. The legend indicates the number of layers in the network. The weights are randomly initialized from a Gaussian distribution. (Left) Weights initialized according to (9). (Right) Weights initialized according to (10).

and identically distributed weights W coming from a rotationally-invariant distribution. To approximately preserve the ℓ_2 norm from the input to the output, we have

$$\sqrt{\mathbb{E}[W^2]} = \sqrt{\frac{2}{(1+a^2)n}}, \quad (10)$$

where n is the number of neurons in the hidden layer.

Note that for small values of a , for example $a = 0.01$, (10) is well approximated by (9). For larger values of a , this approximation breaks down, as shown in Figure 6.

An alternative approach to weight initialization is the data-driven approach [25], which can be applied to more complicated network structures such as convolutional and max-pooling layers commonly used in practice. As parameter distributions change during training, batch normalization inserts layers with learnable scaling and centering parameters at the cost of increased computation and complexity [17].

6.3 Expressivity

Our analysis shows that in a wide MLP with j hidden layers and ReLU activations, some level sets in the weight space can be thought of in terms of the weight distributions in the network. Given a learning task, it should be possible to train only the final layer of a relatively shallow but wide network with different weight distributions and achieve similar results.

This idea is verified as shown in Figure 7. It is interesting to note that despite having different hidden layer distributions, the output layer distributions look very similar after the zeroth training iteration. This supports the theoretical idea that the equivalent kernels in both networks are the same.

Our intention is not to argue that this should be done in practice, merely to verify the existence of level sets in real networks and subnetworks. On the contrary, our results (and in fact, earlier results [7]) can be used to argue against the utility of the controversial so-called Extreme Learning Machine (ELM) [16], which randomly initializes hidden layers from a symmetric distribution and only learns the weights in the final layer. A single layer ELM can be replaced by kernel ridge regression using the equivalent kernel. Furthermore, a Multi-Layer ELM [38] with (L)ReLU activations utilizes a pathological kernel as shown in Figure 5. It should be noted that ELM bears resemblance to earlier works on random neural networks [30, 33].

7 Conclusion

In this paper, we considered certain universal properties of MLPs with (L)ReLU activations and weights coming from a rotationally-invariant distribution. In particular, we, theoretically as well as empirically, showed that the equivalent kernel for networks with an infinite number of hidden ReLU neurons and all rotationally-invariant weight distributions is the Arc-Cosine Kernel. When the activations are LReLUs, the equivalent kernel has a similar form. Empirical results suggest that this result may be generalizable, at least approximately, to the case where f is not rotationally-invariant but only symmetric.

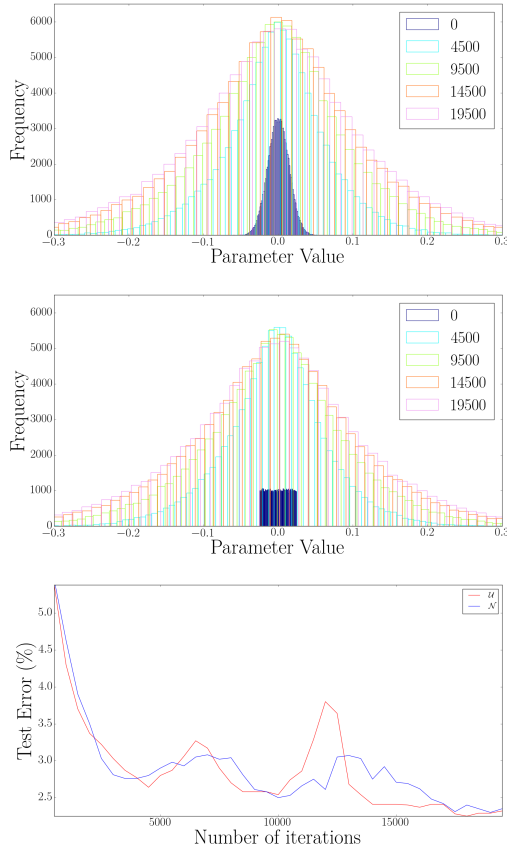


Figure 7: Training only the final layer in a network with 784 inputs, 10000 ReLU hidden units and 10 softmax outputs using a log likelihood cost function on MNIST. The network is trained twice using different initialization schemes, the first where the weights are initialized from a Gaussian distribution and the second where the weights are initialized from a uniform distribution. In both cases the network is optimized using Adam [20] with $\alpha = 0.001$, $\beta_1 = 0.9$ and $\beta_2 = 0.999$ and a batch size of 100. Theano [39] was used. Top: Histograms of final layer parameters during training, hidden layers are Gaussian. Middle: Histograms of final layer parameters during training, hidden layers are uniform. Legend entries indicate number of iterations (number of minibatches seen). Bottom: Test error during training.

One avenue for future work is to study the equivalent kernel for different activation functions, noting that some activations such as the ELU [9] have no guarantee of resulting in a PSD “kernel” or even being expressible as a function of θ_0 with $k(\mathbf{x}, \mathbf{y}) \equiv k(\theta_0)$.

If wide networks with centered symmetric weight distributions have the same equivalent kernel, the expressive power of trained deep and wide MLPs with (L)ReLU activations must lie in the asymmetry and center-offset of the trained network parameter distributions. Another direction for future work is to consider distributions that are not centered around 0, replacing $f(\mathbf{w})$ with $f(\mathbf{w} + \boldsymbol{\mu})$ in (2). Obviously we cannot expect $k(\mathbf{x}, \mathbf{y}) \equiv k(\theta_0)$ in these cases. Empirical investigations of trained network parameter distributions using different optimizer hyperparameters or even different optimizers may yield interesting insights.

A Proof of Proposition 1

Proof. The kernel for an FC layer with weight distribution $f(\boldsymbol{\omega})$ and ReLU activation functions is

$$k(\mathbf{x}, \mathbf{y}) = \int_{\mathbb{R}^m} \Theta(\boldsymbol{\omega} \cdot \mathbf{x}) \Theta(\boldsymbol{\omega} \cdot \mathbf{y}) (\boldsymbol{\omega} \cdot \mathbf{x}) (\boldsymbol{\omega} \cdot \mathbf{y}) f(\boldsymbol{\omega}) d\boldsymbol{\omega}.$$

Let θ_0 be the angle between \mathbf{x} and \mathbf{y} . Define $\mathbf{u} = (\|\mathbf{x}\|, 0, \dots, 0)^T$ and $\mathbf{v} = (\|\mathbf{y}\| \cos \theta_0, \|\mathbf{y}\| \sin \theta_0, 0, \dots, 0)^T$ with $\mathbf{u}, \mathbf{v} \in \mathbb{R}^m$. Following [7], there exists some $m \times m$ rotation matrix R such that $\mathbf{x} = R\mathbf{u}$ and $\mathbf{y} = R\mathbf{v}$. We have

$$k(\mathbf{x}, \mathbf{y}) = \int_{\mathbb{R}^m} \Theta(\boldsymbol{\omega} \cdot R\mathbf{u}) \Theta(\boldsymbol{\omega} \cdot R\mathbf{v}) (\boldsymbol{\omega} \cdot R\mathbf{u}) (\boldsymbol{\omega} \cdot R\mathbf{v}) f(\boldsymbol{\omega}) d\boldsymbol{\omega}.$$

Let $\boldsymbol{\omega} = R\mathbf{w}$ and note that the dot product is invariant under rotations and the determinant of the Jacobian of the transformation is 1 since R is orthogonal. We have

$$\begin{aligned} k(\mathbf{x}, \mathbf{y}) &= \int_{\mathbb{R}^m} \Theta(\mathbf{w} \cdot \mathbf{u})\Theta(\mathbf{w} \cdot \mathbf{v})(\mathbf{w} \cdot \mathbf{u})(\mathbf{w} \cdot \mathbf{v})f(R\mathbf{w}) d\mathbf{w}, \\ &= \int_{\mathbb{R}^m} \Theta(\|\mathbf{x}\|w_1)\Theta(\|\mathbf{y}\|(w_1 \cos \theta_0 + w_2 \sin \theta_0))w_1(w_1 \cos \theta_0 + w_2 \sin \theta_0)f(R\mathbf{w}) d\mathbf{w}\|\mathbf{x}\|\|\mathbf{y}\|. \end{aligned} \quad (11)$$

Using Corollary 7.22 of [19] (which accounts for the distributional nature of the integrand), differentiating twice we have

$$\begin{aligned} \frac{d^2 k}{d\theta_0^2} + k &= \int_{\mathbb{R}^m} \Theta(w_1)w_1(-w_1 \sin \theta_0 + w_2 \cos \theta_0)^2 \delta(w_1 \cos \theta_0 + w_2 \sin \theta_0) f(R\mathbf{w}) d\mathbf{w}\|\mathbf{x}\|\|\mathbf{y}\|, \\ &= \sin \theta_0 \int_{\mathbb{R}^{m-1}} \Theta(s)s^3 f\left(R(s \sin \theta_0, -s \cos \theta_0, w_3, \dots, w_m)^T\right) ds dw_3 dw_4 \dots dw_m \|\mathbf{x}\|\|\mathbf{y}\|. \end{aligned}$$

The initial condition $k(\pi) = 0$ is obtained by putting $\theta_0 = \pi$ in (11) and noting that the resulting integral contains a factor of $\Theta(w_1)\Theta(-w_1)$ which is 0 almost everywhere for any argument. Similarly, $k'(\pi)$ also contains a factor of $\Theta(w_2)\Theta(-w_2)$ in the integrand. \square

B Proof of Proposition 2

Proof. Consider the coefficient of $\sin \theta_0$ in the Fourier series representation of $F(\theta_0)$:

$$\begin{aligned} \langle F, \sin \rangle &= \int_0^{2\pi} \int_{\mathbb{R}^{m-2}} \int_0^\infty \sin^2 \theta_0 s^3 \\ &\quad f\left(R(s \sin \theta_0, -s \cos \theta_0, w_3, \dots, w_m)^T\right) ds dw_3 dw_4 \dots dw_m d\theta_0 \|\mathbf{x}\|\|\mathbf{y}\|, \\ &= \int_{\mathbb{R}^m} w_1^2 f(R\mathbf{w}) d\mathbf{w}\|\mathbf{x}\|\|\mathbf{y}\|, \\ &= \int_{\mathbb{R}^m} \left(\sum_{i=1}^m \alpha_i \omega_i\right)^2 f(\boldsymbol{\omega}) d\boldsymbol{\omega}\|\mathbf{x}\|\|\mathbf{y}\| = \mathbb{E}\left[W_i^2\right] \|\mathbf{x}\|\|\mathbf{y}\|. \end{aligned}$$

The last line is due to uncorrelatedness and the fact that $\|\boldsymbol{\alpha}\| = 1$. So $F(\theta_0) = \frac{\mathbb{E}[W^2]\|\mathbf{x}\|\|\mathbf{y}\|}{\pi} \sin \theta_0 + \frac{a_0}{2} + \sum_{n=1}^\infty a_n \cos(n\theta_0) + \sum_{n=2}^\infty b_n \sin(n\theta_0)$ holds.

To simplify notation we use the following convention: An m_1 dimensional multivariate PDF $f(\mathbf{z})$, $\mathbf{z} \in \mathbb{R}^{m_1}$ will be expressed as $f(\mathbf{z})$, but similarly its marginal $m_2 < m_1$ dimensional multivariate PDF $f(\mathbf{z})$, $\mathbf{z} \in \mathbb{R}^{m_2}$ will be expressed as $f(\mathbf{z})$. The dimensionality of f and its argument will be clear from context.

Due to the rotational invariance of f , we may write $f(O\mathbf{x}) \equiv f(\|\mathbf{x}\|) \equiv f(\mathbf{x})$ for any orthogonal matrix $O \in \mathbf{O}(n)$:

$$\begin{aligned} F(\theta_0) &= \int_{\mathbb{R}^{m-1}} f(R_m(s \sin \theta_0, -s \cos \theta_0, w_3, \dots, w_m)^T) \\ &\quad \sin \theta_0 \Theta(s)s^3 ds dw_3, \dots dw_m \|\mathbf{x}\|\|\mathbf{y}\|, \\ &= \sin \theta_0 \int_{\mathbb{R}} \Theta(s)s^3 f((s \sin \theta_0, -s \cos \theta_0)^T) ds \|\mathbf{x}\|\|\mathbf{y}\|, \\ &= \sin \theta_0 \int_{\mathbb{R}} \Theta(s)s^3 f((s, 0)^T) ds \|\mathbf{x}\|\|\mathbf{y}\|, \\ &= K_2 \sin \theta_0, \quad K_2 \in \mathbb{R}. \end{aligned} \quad (12)$$

By orthogonality, we have that $F(\theta) = \frac{\mathbb{E}[W^2]\|\mathbf{x}\|\|\mathbf{y}\|}{\pi} \sin \theta$. \square

C Proof of Corollary (4)

Proof. It is easy to verify that the LReLU activation function may be expressed as $\sigma(z) = (a + (1 - a)\Theta(z))z$. Expanding out (2), we have

$$\begin{aligned} k(\mathbf{x}, \mathbf{y}) &= \int_{\mathbb{R}^m} \sigma(\mathbf{w} \cdot \mathbf{x})\sigma(\mathbf{w} \cdot \mathbf{y})f(\mathbf{w}) \, d\mathbf{w} \\ &= \int_{\mathbb{R}^m} \left(a^2 + a(1-a)\Theta(\mathbf{w} \cdot \mathbf{y}) + a(1-a)\Theta(\mathbf{w} \cdot \mathbf{x}) + (1-a)^2\Theta(\mathbf{w} \cdot \mathbf{x})\Theta(\mathbf{w} \cdot \mathbf{y}) \right) \\ &\quad (\mathbf{w} \cdot \mathbf{x})(\mathbf{w} \cdot \mathbf{y})f(\mathbf{w}) \, d\mathbf{w} \end{aligned}$$

Using linearity of the integral, we have the superposition of the four integrals

$$\begin{aligned} k_1(\mathbf{x}, \mathbf{y}) &= \int_{\mathbb{R}^m} a^2(\mathbf{w} \cdot \mathbf{x})(\mathbf{w} \cdot \mathbf{y})f(\mathbf{w}) \, d\mathbf{w}, \\ k_2(\mathbf{x}, \mathbf{y}) &= \int_{\mathbb{R}^m} a(1-a)\Theta(\mathbf{w} \cdot \mathbf{y})(\mathbf{w} \cdot \mathbf{x})(\mathbf{w} \cdot \mathbf{y})f(\mathbf{w}) \, d\mathbf{w}, \\ k_3(\mathbf{x}, \mathbf{y}) &= \int_{\mathbb{R}^m} a(1-a)\Theta(\mathbf{w} \cdot \mathbf{x})(\mathbf{w} \cdot \mathbf{x})(\mathbf{w} \cdot \mathbf{y})f(\mathbf{w}) \, d\mathbf{w}, \quad \text{and} \\ k_4(\mathbf{x}, \mathbf{y}) &= \int_{\mathbb{R}^m} (1-a)^2\Theta(\mathbf{w} \cdot \mathbf{x})\Theta(\mathbf{w} \cdot \mathbf{y})(\mathbf{w} \cdot \mathbf{x})(\mathbf{w} \cdot \mathbf{y})f(\mathbf{w}) \, d\mathbf{w}. \end{aligned}$$

Now $k_1(\mathbf{x}, \mathbf{y}) = a^2\sigma_W^2\|\mathbf{x}\|\|\mathbf{y}\|\cos\theta_0$. To see this, rotate the coordinate system as before. Then, either solve the integral directly using the fact that the weights are uncorrelated or differentiate twice and solve the homogeneous IVP with initial conditions $k(0) = a^2\sigma_W^2\|\mathbf{x}\|\|\mathbf{y}\|$ and $k'(0) = 0$.

After rotating the coordinate system, differentiating $k_2(\mathbf{x}, \mathbf{y})$ twice results in a homogeneous IVP with $k(0) = a(1-a)\frac{\sigma_W^2}{2}\|\mathbf{x}\|\|\mathbf{y}\|$ and $k'(0) = 0$, the solution of which is $k_2(\mathbf{x}, \mathbf{y}) = a(1-a)\frac{\sigma_W^2}{2}\|\mathbf{x}\|\|\mathbf{y}\|\cos\theta_0$. Note that by symmetry, $k_2(\mathbf{x}, \mathbf{y}) = k_3(\mathbf{x}, \mathbf{y})$.

The last remaining integral, $k_4(\mathbf{x}, \mathbf{y})$, is just a multiple of the Arc-Cosine kernel.

The sum of all four terms is then

$$k(\mathbf{x}, \mathbf{y}) = \left[\frac{(1-a)^2}{2\pi} (\sin\theta_0 + (\pi - \theta_0)\cos\theta_0) + a\cos\theta_0 \right] \mathbf{E}[W_i^2] \|\mathbf{x}\|\|\mathbf{y}\|.$$

□

D Sampling $F(\theta_0)$

Let us return to $F(\theta_0)$ without assuming a rotationally-invariant f . Examining the i^{th} element of the vector argument of f ,

$$\begin{aligned} (R_m(s \sin \theta_0, -s \cos \theta_0, w_3, \dots, w_m)^T)_i &= \\ (R_{i1} \sin \theta_0 - R_{i2} \cos \theta_0)s + R_{i3}w_3 + \dots + R_{im}w_m, \end{aligned}$$

where R_{ij} represents the element of R_m in the i^{th} row and j^{th} column. Define an $(m) \times (m-1)$ matrix P_{m-1} , constructed by taking R_m and combining the first and second columns through the equation above so that

$$\begin{aligned} &R_m(s \sin \theta_0, -s \cos \theta_0, w_3, \dots, w_m)^T \\ &= P_{m-1}(s, w_3, \dots, w_m)^T. \end{aligned}$$

Note that the rank of P_{m-1} is $m-1$. Define T_{m-1} to be the $(m-1) \times (m-1)$ matrix containing the first $m-1$ rows of P_{m-1} . Due to linear dependence, and assuming the weights are independent, we have

$$\begin{aligned} &f(R_m(s \sin \theta_0, -s \cos \theta_0, w_3, \dots, w_m)^T) \\ &= f(T_{m-1}(s, w_3, \dots, w_m)^T) f\left(\sum_{i=1}^{m-1} \gamma_i \mathbf{t}_i \cdot (s, w_3, \dots, w_m)^T\right), \end{aligned}$$

where \mathbf{t}_i is the i^{th} row of T_{m-1} and $\gamma_i \in \mathbb{R}$ with $T_{m-1}^T \boldsymbol{\gamma} = (\mathbf{p}_m)^T$ where \mathbf{p}_m is the m^{th} row of P_{m-1} .

Let τ_1 denote the first row of T_{m-1}^{-1} and \mathbf{W}_{m-1} denote the $m - 1$ dimensional random weight vector. Making the substitution $T_{m-1}^{-1}\boldsymbol{\omega} = (s, w_3, \dots, w_m)^T$,

$$\begin{aligned}
F(\theta_0) &= \sin \theta_0 \int_{\mathbb{R}^{m-1}} \Theta(s) s^3 f(T_{m-1}(s, w_3, \dots, w_m)^T) f\left(\sum_{i=1}^{m-1} \gamma_i \mathbf{t}_i \cdot (s, w_3, \dots, w_m)^T\right) \\
&\quad ds dw_3, \dots, dw_m \|\mathbf{x}\| \|\mathbf{y}\|, \\
&= \frac{\sin \theta_0}{|\det(T_{m-1})|} \int_{\mathbb{R}^{m-1}} \Theta(\boldsymbol{\tau}_1 \cdot \boldsymbol{\omega}_{m-1}) (\boldsymbol{\tau}_1 \cdot \boldsymbol{\omega}_{m-1})^3 f(\boldsymbol{\omega}_{m-1}) f\left(\sum_{i=1}^{m-1} \gamma_i \omega_i\right) d\boldsymbol{\omega}_{m-1} \|\mathbf{x}\| \|\mathbf{y}\|, \\
&= \frac{\sin \theta_0}{|\det(T_{m-1})|} \mathbb{E} \left[\Theta(\mathbf{W}_{m-1} \cdot \boldsymbol{\tau}_1) (\mathbf{W}_{m-1} \cdot \boldsymbol{\tau}_1)^3 f(\boldsymbol{\gamma} \cdot \mathbf{W}_{m-1}) \right] \|\mathbf{x}\| \|\mathbf{y}\|, \\
&= \frac{\sin \theta_0}{2|\det(T_{m-1})|} \mathbb{E} \left[f(\boldsymbol{\gamma} \cdot \mathbf{W}_{m-1}) \left((\mathbf{W}_{m-1} \cdot \boldsymbol{\tau}_1)^3 + |(\mathbf{W}_{m-1} \cdot \boldsymbol{\tau}_1)|^3 \right) \right] \|\mathbf{x}\| \|\mathbf{y}\|,
\end{aligned}$$

where the last line uses the identity $\Theta(z)z = \frac{1}{2}(|z| + z)$.

References

- [1] Francis Bach. Breaking the curse of dimensionality with convex neural networks. *Journal of Machine Learning Research*, 18(19):1–53, 2017.
- [2] David Balduzzi, Marcus Frean, Lennox Leary, J. P. Lewis, Kurt Wan-Duo Ma, and Brian McWilliams. The shattered gradients problem: If resnets are the answer, then what is the question? In *Proceedings of the 34th International Conference on Machine Learning*, volume 70, pages 342–350, 2017.
- [3] Yoshua Bengio, Patrice Simard, and Paolo Frasconi. Learning long-term dependencies with gradient descent is difficult. *IEEE transactions on neural networks*, 5(2):157–166, 1994.
- [4] David Berthelot, Tom Schumm, and Luke Metz. Began: Boundary equilibrium generative adversarial networks. *arXiv preprint arXiv:1703.10717*, 2017.
- [5] Wlodzimierz Bryc. Rotation invariant distributions. In *The Normal Distribution*, pages 51–69. Springer, 1995.
- [6] A Neil Burgess. Estimating equivalent kernels for neural networks: A data perturbation approach. In *Advances in Neural Information Processing Systems*, pages 382–388, 1997.
- [7] Youngmin Cho and Lawrence K Saul. Kernel methods for deep learning. In *Advances in neural information processing systems*, pages 342–350, 2009.
- [8] Anna Choromanska, Mikael Henaff, Michael Mathieu, Gérard Ben Arous, and Yann LeCun. The loss surfaces of multilayer networks. In *Artificial Intelligence and Statistics*, pages 192–204, 2015.
- [9] Djork-Arné Clevert, Thomas Unterthiner, and Sepp Hochreiter. Fast and accurate deep network learning by exponential linear units (elus). In *ICLR*, 2016.
- [10] Amit Daniely, Roy Frostig, and Yoram Singer. Toward deeper understanding of neural networks: The power of initialization and a dual view on expressivity. In *Advances In Neural Information Processing Systems*, pages 2253–2261, 2016.
- [11] Xavier Glorot and Yoshua Bengio. Understanding the difficulty of training deep feedforward neural networks. In *Proceedings of the Thirteenth International Conference on Artificial Intelligence and Statistics*, pages 249–256, 2010.
- [12] Benjamin D Haeffele and René Vidal. Global optimality in tensor factorization, deep learning, and beyond. *arXiv preprint arXiv:1506.07540*, 2015.
- [13] Kaiming He, Xiangyu Zhang, Shaoqing Ren, and Jian Sun. Delving deep into rectifiers: Surpassing human-level performance on imagenet classification. In *Proceedings of the IEEE international conference on computer vision*, pages 1026–1034, 2015.
- [14] Sepp Hochreiter. Untersuchungen zu dynamischen neuronalen netzen. *Diploma, Technische Universität München*, 91, 1991.

- [15] Sepp Hochreiter, Yoshua Bengio, and Paolo Frasconi. Gradient flow in recurrent nets: the difficulty of learning long-term dependencies. In J. Kolen and S. Kremer, editors, *Field Guide to Dynamical Recurrent Networks*. IEEE Press, 2001.
- [16] Guang-Bin Huang, Qin-Yu Zhu, and Chee-Kheong Siew. Extreme learning machine: a new learning scheme of feedforward neural networks. In *Neural Networks, 2004. Proceedings. 2004 IEEE International Joint Conference on*, volume 2, pages 985–990. IEEE, 2004.
- [17] Sergey Ioffe and Christian Szegedy. Batch normalization: Accelerating deep network training by reducing internal covariate shift. In *International Conference on Machine Learning*, pages 448–456, 2015.
- [18] Mark E Johnson. *Multivariate statistical simulation: A guide to selecting and generating continuous multivariate distributions*. John Wiley & Sons, 2013.
- [19] D. S. Jones. *The Theory of Generalised Functions*, chapter 7, page 233. Cambridge University Press, 2nd edition, 1982.
- [20] Diederik Kingma and Jimmy Ba. Adam: A method for stochastic optimization. In *International Conference on Learning Representations*, 2015.
- [21] Jaehoon Lee, Yasaman Bahri, Roman Novak, Schoenholz Samuel S, Jeffrey Pennington, and Jascha Sohl-Dickstein. Deep neural networks as gaussian processes. *arXiv preprint arXiv:1611.01232*, 2017.
- [22] Roi Livni, Daniel Carmon, and Amir Globerson. Learning infinite layer networks without the kernel trick. In *International Conference on Machine Learning*, pages 2198–2207, 2017.
- [23] David JC MacKay. A practical bayesian framework for backpropagation networks. *Neural computation*, 4(3):448–472, 1992.
- [24] Charles H Martin and Michael W Mahoney. Rethinking generalization requires revisiting old ideas: statistical mechanics approaches and complex learning behavior. *arXiv preprint arXiv:1710.09553*, 2017.
- [25] Dmytro Mishkin and Jiri Matas. All you need is a good init. In *International Conference on Learning Representations*, 2016.
- [26] Radford M Neal. *Bayesian Learning for Neural Networks*. PhD thesis, University of Toronto, 1994.
- [27] Aaron van den Oord, Sander Dieleman, Heiga Zen, Karen Simonyan, Oriol Vinyals, Alex Graves, Nal Kalchbrenner, Andrew Senior, and Koray Kavukcuoglu. Wavenet: A generative model for raw audio. *arXiv preprint arXiv:1609.03499*, 2016.
- [28] Gaurav Pandey and Ambedkar Dukkipati. Learning by stretching deep networks. In *Proceedings of the 31st International Conference on Machine Learning (ICML-14)*, pages 1719–1727, 2014.
- [29] Gaurav Pandey and Ambedkar Dukkipati. To go deep or wide in learning? In *Artificial Intelligence and Statistics*, pages 724–732, 2014.
- [30] Yoh-Han Pao, Gwang-Hoon Park, and Dejan J Sobajic. Learning and generalization characteristics of the random vector functional-link net. *Neurocomputing*, 6(2):163–180, 1994.
- [31] Ben Poole, Subhaneil Lahiri, Maithreyi Raghu, Jascha Sohl-Dickstein, and Surya Ganguli. Exponential expressivity in deep neural networks through transient chaos. In *Advances In Neural Information Processing Systems*, pages 3360–3368, 2016.
- [32] Maithra Raghu, Ben Poole, Jon Kleinberg, Surya Ganguli, and Jascha Sohl-Dickstein. On the expressive power of deep neural networks. In Doina Precup and Yee Whye Teh, editors, *Proceedings of the 34th International Conference on Machine Learning*, volume 70 of *Proceedings of Machine Learning Research*, pages 2847–2854, 2017.
- [33] Wouter F Schmidt, Martin A Kraaijveld, and Robert PW Duin. Feedforward neural networks with random weights. In *Pattern Recognition, 1992. Vol. II. Conference B: Pattern Recognition Methodology and Systems, Proceedings., 11th IAPR International Conference on*, pages 1–4. IEEE, 1992.
- [34] Samuel S Schoenholz, Justin Gilmer, Surya Ganguli, and Jascha Sohl-Dickstein. Deep information propagation. In *International Conference on Learning Representations*, 2017.

- [35] Ravid Shwartz-Ziv and Naftali Tishby. Opening the Black Box of Deep Neural Networks via Information. *arXiv preprint arXiv:1703.00810*, 2017.
- [36] David Silver, Julian Schrittwieser, Karen Simonyan, Ioannis Antonoglou, Aja Huang, Arthur Guez, Thomas Hubert, Lucas Baker, Matthew Lai, Adrian Bolton, et al. Mastering the game of go without human knowledge. *Nature*, 550(7676):354–359, 2017.
- [37] Aman Sinha and John C Duchi. Learning kernels with random features. In *Advances in Neural Information Processing Systems*, pages 1298–1306, 2016.
- [38] Jiexiong Tang, Chenwei Deng, and Guang-Bin Huang. Extreme learning machine for multilayer perceptron. *IEEE transactions on neural networks and learning systems*, 27(4):809–821, 2016.
- [39] Theano Development Team. Theano: A Python framework for fast computation of mathematical expressions. *arXiv e-prints*, abs/1605.02688, May 2016.
- [40] Christopher KI Williams. Computing with infinite networks. In *Advances in neural information processing systems*, pages 295–301, 1997.
- [41] Chiyuan Zhang, Samy Bengio, Moritz Hardt, Benjamin Recht, and Oriol Vinyals. Understanding deep learning requires rethinking generalization. *arXiv preprint arXiv:1611.03530*, 2016.